Optical Imaging of Electrical Carrier Injection into Individual InAs Quantum Dots

A. Baumgartner,[1,*] E. Stock,[2] A. Patanè,[1] L. Eaves,[1] M. Henini,[1] and D. Bimberg[2]
[1]School of Physics and Astronomy, University of Nottingham, Nottingham NG7 2RD, United Kingdom
[2]Technical University Berlin, Hardenbergstrasse 36, 10623 Berlin, Germany
(Received 15 July 2010; published 13 December 2010)

We image the micro-electroluminescence (EL) spectra of self-assembled InAs quantum dots (QDs) embedded in the intrinsic region of a GaAs *p-i-n* diode and demonstrate optical detection of carrier injection into a single QD. Tunneling of electrons and holes into the QDs at bias voltages below the flat-band condition leads to a spectrum of sharp EL lines from a small number of bright spots on the diode surface, characteristic of emission from individual QDs. We explain this behavior in terms of Coulomb interaction effects and the selective excitation of a small number of QDs within the ensemble due to preferential tunneling paths for carriers.

DOI: 10.1103/PhysRevLett.105.257401 PACS numbers: 78.67.Hc, 73.21.La, 73.63.-b, 78.60.Fi

Self-assembled InAs quantum dots (QDs) are an important model system for investigating the fundamental physics of quantum-confined electrons [1–3]. The selective light emission from a small number of QDs can be achieved, for example, by lithographically defined small-area diodes [4] or apertures [5], or by the incorporation of QDs into microcavities [6,7] and nanowires [8,9]. Such studies have provided information about the electronic properties of the dots and form the basis for novel applications, e.g., optically [10] and electrically [11] driven sources of entangled photon pairs for quantum information processing. Of particular interest is the possibility of generating sharp electroluminescence (EL) emission lines from individual QDs by voltage controlled electrical injection of carriers. Despite many works on resonant tunneling injection of carriers in unipolar QD devices [12–15], the simultaneous resonant injection of both electrons and holes required for EL emission from an individual QD has received less attention [16,17], yet it is relevant to topical research on electrically driven single-QD photon emitters [11].

Here we use micro-electroluminescence (μEL) spectroscopy and imaging to investigate the optical emission from a single layer of self-assembled InAs quantum dots embedded in the intrinsic region of a *p-i-n* light emitting diode. By gradually decreasing the applied bias below the ''flat band'' threshold voltage at which the bias balances the built-in potential in the *i* region, we follow the evolution of the EL spectra and the corresponding spatial form of the EL emission. With decreasing bias the EL spectrum evolves into a series of sharp EL lines characteristic of single QDs. At the same time, the EL becomes confined to a small number of bright emission spots, each with its own spectral fingerprint and Stark shift. We attribute this behavior to the existence of preferential pathways through which carriers can tunnel into only a small number of dots within the large ensemble. We exploit this phenomenon to reveal the resonant tunneling excitation of a small number of individual QDs. This demonstration of bias-controlled tunneling excitation of EL has potential for use in optoelectronic and quantum information applications.

Our *p-i-n* diodes were grown by molecular beam epitaxy on a p^+ GaAs substrate, which forms the bottom electrical contact of the diode. The layer structure in order of growth on the substrate is as follows: a 200 and a 50 nm *p*-doped GaAs layers with $p = 4 \times 10^{18}$ cm^{-3} and $p = 5 \times 10^{17}$ cm^{-3}, respectively; a 6 nm intrinsic GaAs spacer layer; a 1.8 monolayer (ML) of InAs, which gives rise to a wetting layer (WL) and the QDs with a density of about 10^{10} cm^{-2}. The QD layer is covered by 16 nm of intrinsic GaAs followed by 50 nm *n*-doped GaAs ($n = 2 \times 10^{16}$ cm^{-3}) and a 500 nm GaAs top layer with $n = 4 \times 10^{18}$ cm^{-3}. The diodes are defined by wet-chemical etching and a ring-shaped gold electrode forms the top electrical contact and provides optical access. Here we focus on large-area devices with 200 μm diameter, containing $\sim 10^6$ QDs. A schematic band diagram for a bias U below the flat-band condition, i.e., for $U < 1.5$ V, is shown in the inset of Fig. 1(a). The μEL spectra were recorded at $T \approx 15$ K with a spectral resolution of ~ 40 μeV and a focal spot diameter of about 20 μm. The spatial maps of the μEL were recorded by scanning the focusing mirror along the mesa.

Figure 1(a) shows the EL spectra for a range of applied biases U. As U is decreased below the flat-band condition, the EL spectrum narrows and evolves into single sharp lines. To track the evolution of the EL spectrum with U, we show in Fig. 1(b) a color-scale plot of the normalized EL intensity versus U and the photon energy, $h\nu$. This reveals the narrowing of the QD emission with decreasing bias and the emergence of two distinct features *A* and *B* emphasized by dashed lines in Fig. 1(b). Both features shift to lower energies with decreasing bias with peak energies that run parallel to the line $eU = h\nu$. The energy difference

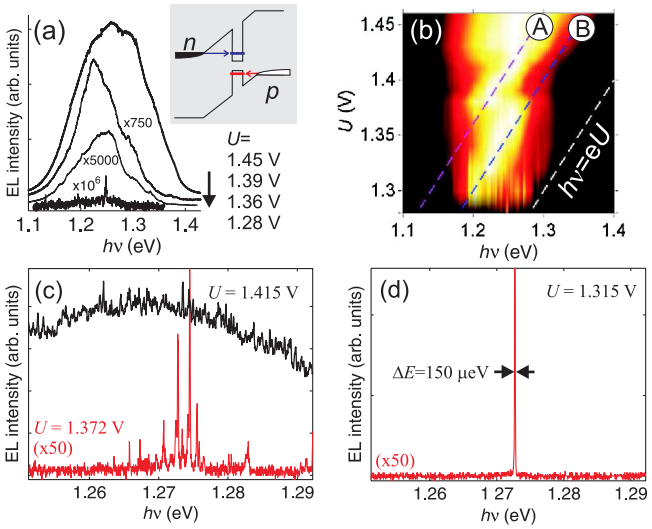

FIG. 1 (color online). (a) EL spectra of the diode for a series of bias voltages U. Inset: schematic diagram of the resonant injection of electrons and holes into a QD. (b) Color scale image of the normalized EL intensity as a function of photon energy and bias. The dashed lines represent the conditions $eU = h\nu$, $eU = h\nu + 100$ meV and $eU = h\nu + 160$ meV. (c) and (d) μEL spectra showing the fragmentation of the continuous EL spectrum into a sharp emission line.

between the excitation energy eU and the peak energy of each feature is $E_A = 160$ meV and $E_B = 100$ meV, respectively. This indicates that electron-hole pairs are created by electrical injection into two different excited states A and B of the QDs, and that they relax an energy of E_A and E_B prior to the radiative recombination in the ground state.

We now focus on the μEL spectra in the energy interval $1.25\ \text{eV} < h\nu < 1.29\ \text{eV}$ at low applied bias. Figures 1(c) and 1(d) show the μEL spectrum at a given position on the mesa at different U. With decreasing U the spectrum evolves from a broad continuous emission into a fragmented spectrum. At $U = 1.315$ V the emission consists of a single sharp line only, with a full width at half maximum of ~ 150 μeV. This linewidth is not determined by the resolution of the spectrometer and is similar to the typical linewidths reported for the low temperature photoluminescence emission of individual InAs QDs [18]. This method of EL excitation allows the study of such sharp emission lines over several orders of magnitudes in intensity and also reveals a characteristic exponential acoustic phonon broadening and a weak but sharp phonon replica peak, reported elsewhere [19].

The evolution of the EL spectrum into sharp lines with decreasing bias is accompanied by a spatial fragmentation of the surface EL emission into a series of bright spots. To demonstrate this effect, we recorded μEL spectra at each position of a square grid covering roughly $1/4$ of the diode surface. Figure 2 shows spatial maps of the maximum intensity of each spectrum as a function of position for a series of bias voltages. For each image, a scale factor relates the maximum of the color scale to the maximum at $U = 1.415$ V.

At $U = 1.415$ V the emission is essentially homogeneous across the scan [20]. At a slightly lower bias, $U = 1.395$ V, the diode emission starts to break up into a series of bright spots dominating over a homogeneous background emission. At $U = 1.385$ V, the background intensity weakens and several bright spots emerge at distinct positions with a uniform spot size determined by the diameter of the focal spot of the collecting lens. At this voltage the EL spectra fragment into sharp lines. At $U = 1.372$ V, the number of bright spots decreases and the relative intensities of the individual spots change compared to the image at $U = 1.385$ V. The spectra now consist of individual emission lines with no background EL. At $U = 1.345$ V, the maximum intensities are much lower and the number of visible emission spots is reduced to four. At $U = 1.315$ V, only one bright spot is visible and the corresponding spectrum, shown in Fig. 1(d), consists of a single sharp emission line with an intensity similar to the maximum at $U = 1.372$ V. We note that no other EL lines could be observed at this bias, suggesting that this emission center originates from a single QD.

The EL spectra corresponding to the spatial EL maps are presented in Fig. 3 for $U = 1.372$ V. Figure 3(a) shows maps of the normalized EL intensity as a function of position at specific photon energies. The individual scans are distinguished by different colors and the corresponding energies are indicated by arrows in the μEL spectra of Fig. 3(b). The bright spots in Fig. 3(a) and the corresponding EL spectra of Fig. 3(b) are labeled as P1-P7. Each spot has approximately the same size and circular shape as the one that gives rise to the sharp EL emission in Fig. 1(d) and

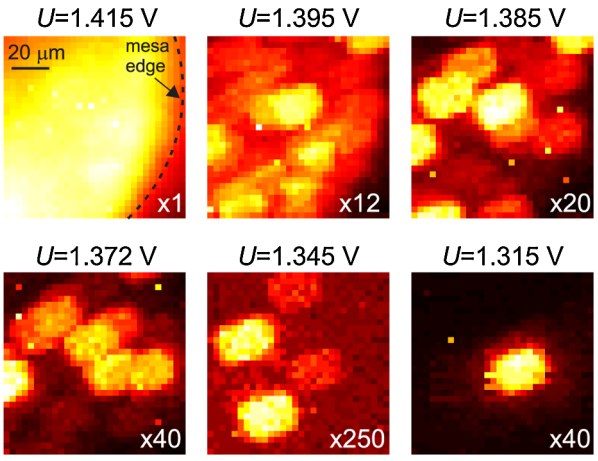

FIG. 2 (color online). Maps of the maximum surface μEL intensity for a range of applied biases. For a given bias the EL spectrum is recorded for a grid of positions. The images show the maximum intensity of each spectrum as a function of the position on the diode. The number at the bottom right of each image denotes the factor by which the EL intensity is scaled compared to the first image.

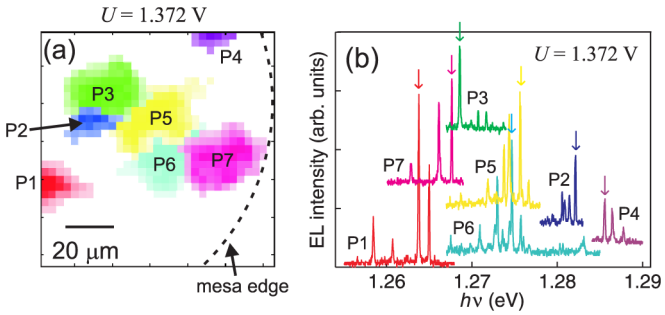

FIG. 3 (color online). (a) Overlay image of several μEL intensity maps at different photon energies, given by arrows of the same color in (b). The symbols P1-P7 mark the position of the maximum EL intensity at this energy. Features with intensities below the threshold of 10% of the maximum in a scan are omitted for clarity. (b) EL spectra recorded for $U = 1.372$ V at the positions P1-P7 given in (a). The EL spectra are offset for clarity.

has a unique spectral fingerprint consisting of a small number of sharp lines. In turn, each emission line originates from exactly one bright spot in the spatial scans [21]. These observations are consistent with the selective excitation of a small number of dots by carriers tunneling in the area of the bright spots.

Figure 4(a) shows the bias dependence of the peak intensity of the emission line L1 of Fig. 1(d) at the energy $h\nu = 1.2730$ eV. The EL intensity exhibits sharp peaks at bias voltages of $U = 1.32$ V and $U = 1.37$ V. These resonances are a manifestation of the voltage-tunable resonant tunneling excitation of a single QD detected by optical means. The resonant injection of carriers from the doped contact layers into discrete excited states of the QD is followed by energy relaxation into the ground state and radiative recombination. The two bias resonances are separated in energy by ~56 meV and the differences from the ground state energy are 42 and 99 meV, both typical values for the quantum confinement energies of self-assembled InAs QDs. For $U > 1.4$ V the strong growth of the EL intensity arises from an increasing contribution of the emission from the QD ensemble, which is excited through carrier injection and redistribution into the extended states of the wetting layer and of the GaAs matrix as the flat-band condition is approached [22]. We find resonances on several other sharp EL lines in this spectral range, though the number of observed resonances and their amplitudes can differ, as shown for the lines L4 and L5 in Fig. 4(a).

The emission energy of individual EL lines depends on the applied bias, as can be seen in Fig. 4(b), where the energy shift ΔE relative to the value at $U = 1.41$ V is plotted for several lines L1–L5. We attribute this bias dependence to the quantum-confined Stark effect in the QD [23,24]. Of particular interest is that the energies of some of the lines remain constant over certain bias ranges. For example, line L1 does not shift between ~1.36 and 1.38 V, suggesting that the electric field in the intrinsic region remains constant. We propose that an imbalance between electron and hole tunneling in this bias interval increases the average charge density in the QD layer, thus screening the local electric field, an effect analogous to the charge buildup reported previously for resonant tunneling quantum well diodes [25]. Also note that, although the Stark shifts for various EL lines differ from each other, the rates of shift with bias are very similar. This indicates that the different bias dependences arise from mesoscopic variations of the potential landscape rather than from differences in the electronic properties of the QDs.

Our data demonstrate that at low temperatures the EL emission of some QDs can be excited by resonant tunneling injection of carriers into the excited states of the QD. The electrons and holes in the n- and p-type layers close to the QDs have an energy spread given by the respective Fermi energies (< 10 meV). Since both the electron and hole states have to be aligned with the Fermi seas for tunneling, one would expect considerably narrower bias resonances than the ones reported here. On the other hand, the Coulomb interaction of a charged QD with the Fermi seas of the contacts and with its nearest neighbor QDs can provide additional tunneling pathways, thus accounting for the relatively large widths (> 10 mV) of the resonances in Fig. 4(a). We note that this broadening is significantly larger than the width of individual QD EL lines (~ 150 μeV).

Though the number of active QDs is constrained by the conditions of resonant tunneling, this constraint is not sufficient to explain the pronounced spectral and spatial fragmentation of the EL emission revealed in our study. Existing theoretical models [16] do not predict such an effect either. The high density and uniform distribution of QDs ensures that even at the lowest bias several dots could be active. Hence we conclude that some dots are coupled more strongly to the reservoirs than others, which is supported by the different number of observable resonances for different QDs shown in Fig. 4(a). Since the emission energies of the investigated QDs are very similar, this variation of the coupling is likely to be due to local variations of the tunnel distance and barrier height. In previous studies, μEL maps of the emission from the

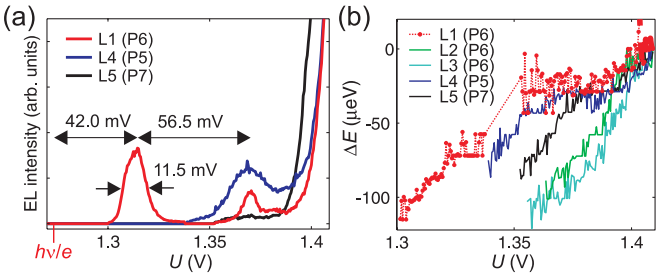

FIG. 4 (color online). (a) Peak intensity of the L1, L4, and L5 lines as a function of bias. The arrows show the energy separation of two resonances from the energy of the L1 line. (b) Energy shift of several EL lines as a function of bias. P5, P6, and P7 correspond to the positions on the mesa given in Fig. 3(a).

ridge-waveguide regions of InGaN quantum well based LEDs have revealed spatial inhomogeneities due to nonuniform carrier injection caused by crystal degradation [26]. In our diodes, the EL spectra are stable with time, but preferential tunneling paths may arise from mesoscopic fluctuations of the n- and p-doped interfaces due to randomly placed dopant atoms in or close to the intrinsic region, crystals defects or strain-related potential minima associated with the QDs themselves. Such variations would not only explain the spatial and spectral fragmentation of the EL spectra, but could also account for some differences in the bias dependence of the Stark shifts among various QDs.

In summary, we have demonstrated how the homogeneous broadband emission of a large quantum dot ensemble evolves into spatially inhomogeneous sharp emission lines from individual quantum dots with decreasing bias. The peak intensity of many of the sharp EL lines exhibits a distinct resonance behavior as a function of the applied bias and a unique Stark shift. These effects can be explained in terms of the selective excitation of a small number of QDs within the ensemble due to the presence of preferential tunneling paths for carriers. We note that single EL lines are observed at low bias when the current is typically 5 orders of magnitude smaller than for the excitation of the whole QD ensemble at the flat-band threshold. Under these conditions, most of the QDs are empty, thus reducing quantum decoherence due to Coulomb interactions between the active QDs and their neighbors. Decoherence could be further reduced by using diodes with a lower density of QDs. Our results provide direct evidence for the voltage-tunable electrical injection of carriers into individual QDs, which is relevant for the realization of electrically driven single-QD photon sources. They could be implemented in a broad range of optoelectronic materials and are of interest to the growing community of researchers studying the physics and applications of quantum information processing.

This work is supported by the Engineering and Physical Sciences Research Council (UK) and the Deutsche Forschungsgemeinschaft in the frame of SFB 787.

*andreas.baumgartner@unibas.ch
Present address: Nanoelectronics Group, University of Basel, Switzerland.

[1] A. D. Yoffe, Adv. Phys. **50**, 1 (2001).
[2] D. Bimberg, Electron. Lett. **44**, 168 (2008).
[3] N. N. Ledentsov *et al.*, J. Lightwave Technol. **26**, 1540 (2008).
[4] J.-Y. Marzin *et al.*, Phys. Rev. Lett. **73**, 716 (1994).
[5] Z. Yuan *et al.*, Science **295**, 102 (2001).
[6] P. Michler *et al.*, Science **290**, 2282 (2000).
[7] M. Nomura *et al.*, Nature Phys. **6**, 279 (2010).
[8] N. Panev *et al.*, Appl. Phys. Lett. **83**, 2238 (2003).
[9] J. Claudon *et al.*, Nat. Photon. **4**, 174 (2010).
[10] R. M. Stevenson *et al.*, Nature (London) **439**, 179 (2006).
[11] C. L. Salter *et al.*, Nature (London) **465**, 594 (2010).
[12] M. Narihiro *et al.*, Appl. Phys. Lett. **70**, 105 (1997).
[13] I. Hapke-Wurst *et al.*, Phys. Rev. B **62**, 12621 (2000).
[14] A. Patanè *et al.*, Phys. Rev. B **65**, 165308 (2002).
[15] D. Reuter *et al.*, Phys. Rev. Lett. **94**, 026808 (2005).
[16] G. Kiesslich *et al.*, Phys. Rev. B **68**, 125331 (2003).
[17] L. Turyanska *et al.*, Appl. Phys. Lett. **89**, 092106 (2006).
[18] G. Ortner *et al.*, Phys. Rev. B **70**, 201301(R) (2004).
[19] E. Stock *et al.*, *Conference on Lasers and Electro-Optics, and Quantum Electronics and Laser Science Conference (CLEO/QELS 2009)*, Vol. 1–5, p. 2418 (IEEE, New York, 2009).
[20] The large scale deviations in the image are mainly due to a misalignment of the focal plane of the lens and the sample surface.
[21] A small number of weak emission lines occur in more than one spectrum due to stray light from overlapping collection areas.
[22] A. Baumgartner *et al.*, Appl. Phys. Lett. **92**, 091121 (2008).
[23] P. W. Fry, I. E. Itskevich *et al.*, Phys. Rev. Lett. **84**, 733 (2000).
[24] A. Patanè *et al.*, Appl. Phys. Lett. **77**, 2979 (2000).
[25] M. L. Leadbeater *et al.*, J. Phys. Condens. Matter **1**, 10605 (1989).
[26] M. Rossetti *et al.*, Appl. Phys. Lett. **92**, 151110 (2008).